Electronic Supplementary Material (ESI) for Materials Horizons.

Supporting Information:

A Highly Sensitive Graphene Woven Fabric Strain Sensor for Wearable Wireless Musical Instrument

Xu Liu[1], Chen Tang[1], Xiaohan Du[1], Shuai Xiong[1], Siyuan Xi[1], Yuefeng Liu[1], Xi Shen[1], Qingbin Zheng[1,2,], Zhenyu Wang[1], Ying Wu[1], Andrew Horner[3], and Jang-Kyo Kim[1,*]*

[1] Department of Mechanical and Aerospace Engineering, The Hong Kong University of Science and Technology, Clear Water Bay, Kowloon, Hong Kong

[2] Institute for Advanced Study, The Hong Kong University of Science and Technology, Clear Water Bay, Hong Kong

[3] Department of Computer Science and Engineering, The Hong Kong University of Science and Technology, Clear Water Bay, Hong Kong

*Corresponding author: Fax: +852 2358 1543; email: mezheng@ust.hk (QB Zheng) mejkkim@ust.hk (J-K Kim)

S1. Measurements of strains in composites and GTs

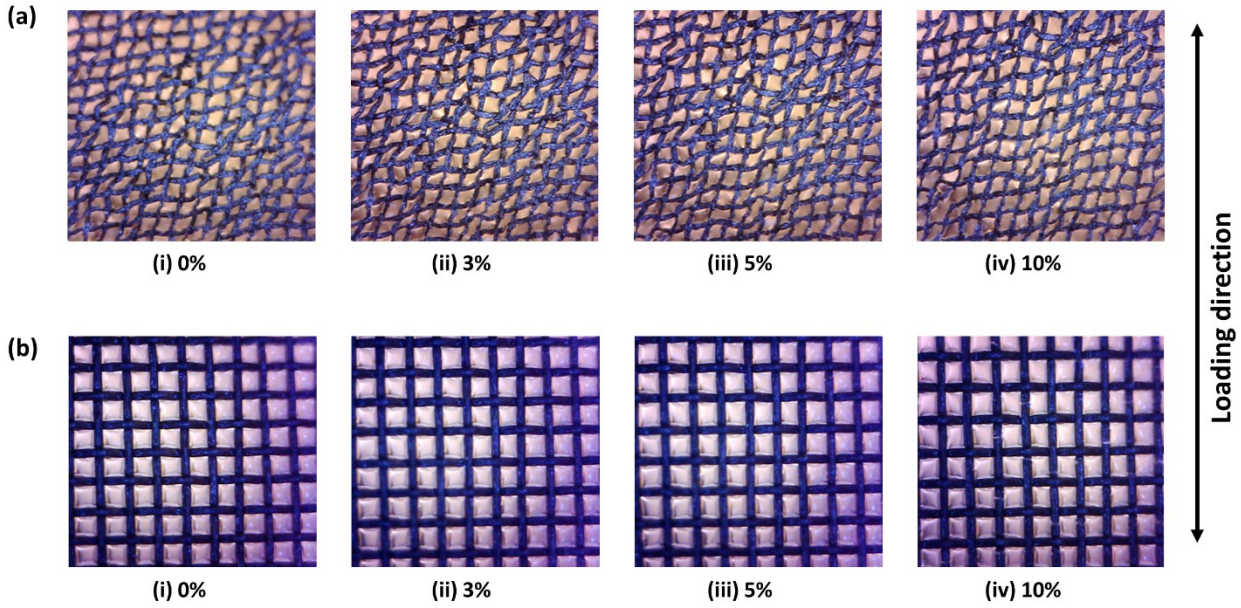

Figure S1 Optical images of GWF/PDMS composites with GWFs grown under (a) 3.0 and (b) 10.0 vol% CH_4 at different tensile strains.

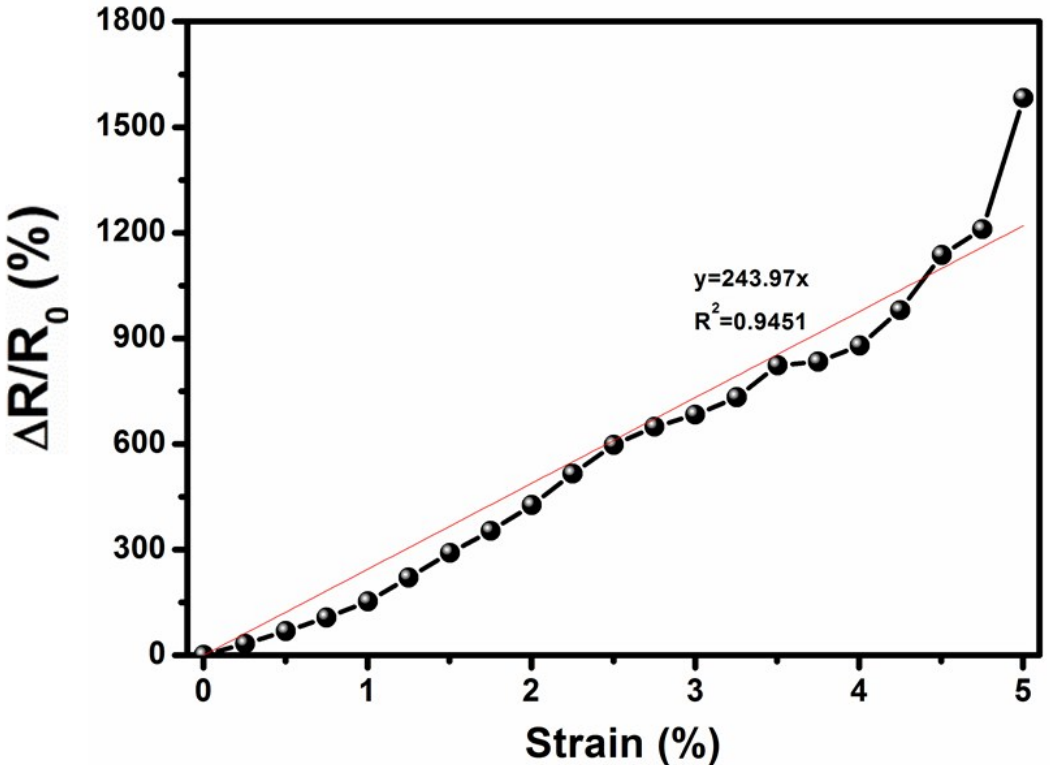

Figure S2 Normalized resistance change of GWF/PDMS composites as a function of applied tensile strain (0-5%).

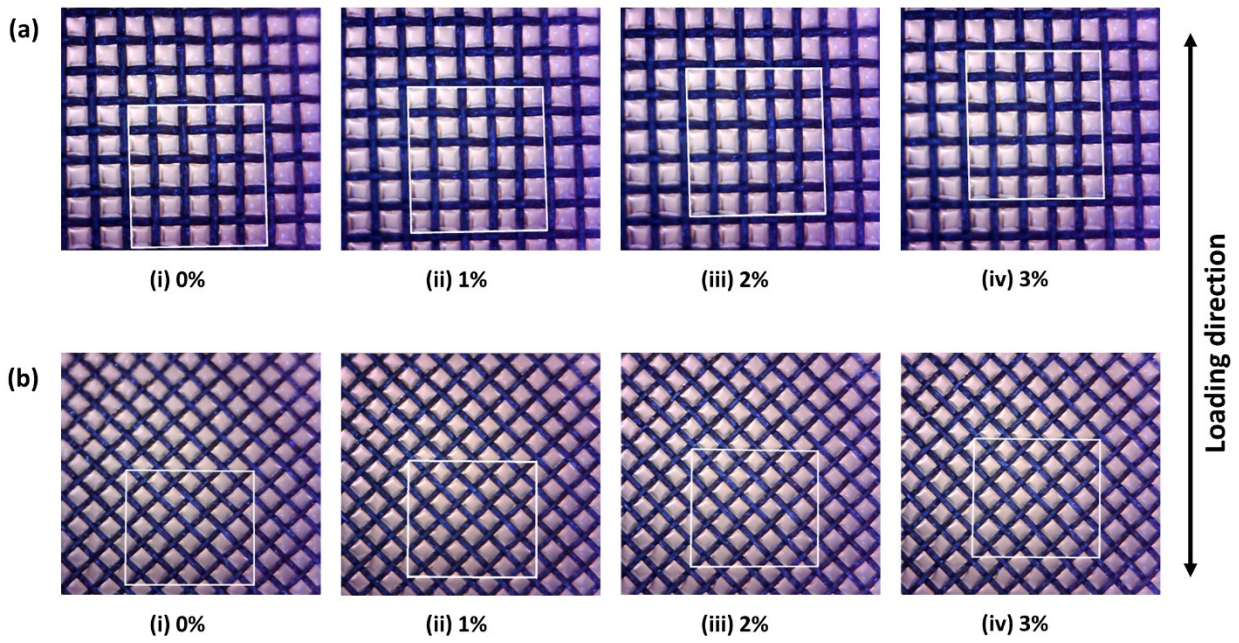

Figure S3 Optical images of GWF/PDMS composites with GTs oriented at (a) 0° and (b) 45° taken at different tensile strains.

S2. Calculation of resistance change of composite using a simplified circuit model

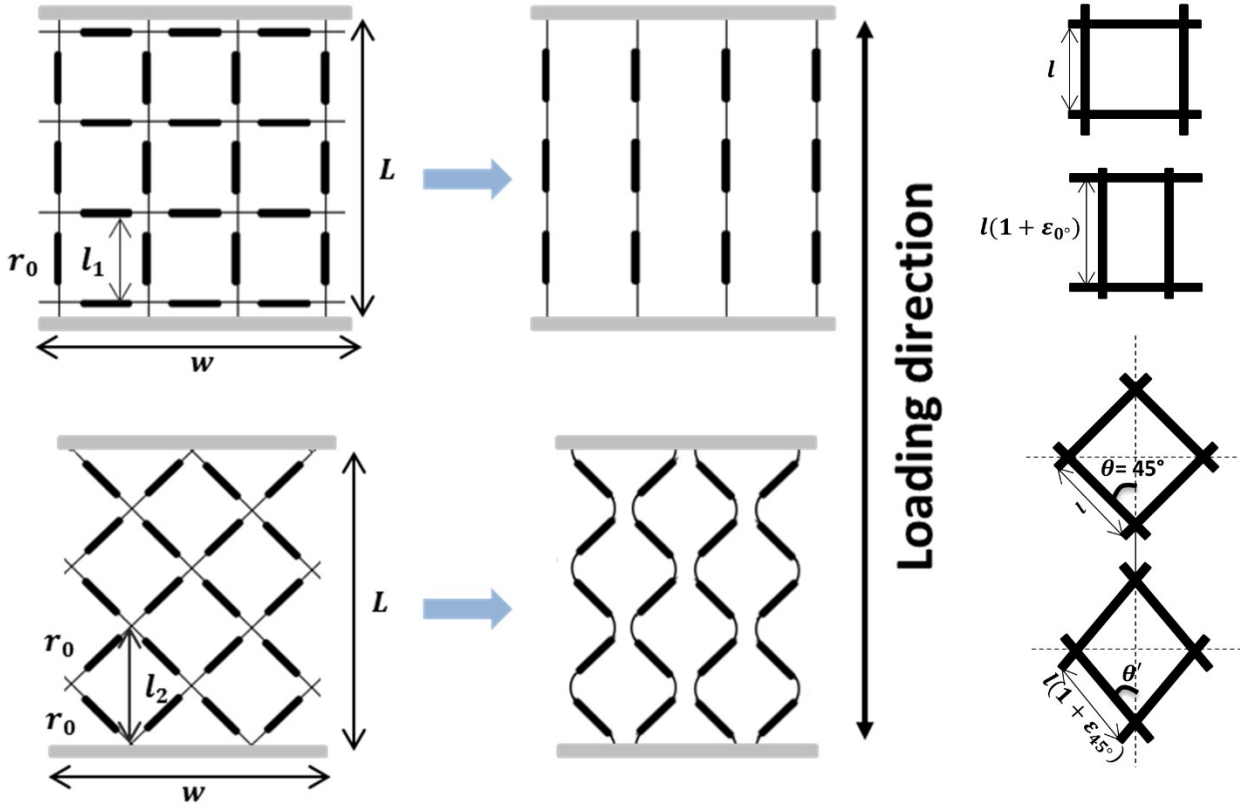

Figure S4 Equivalent and simplified circuit models for estimating the resistance change in GWF networks with GTs oriented 0° and 45° to the loading direction.

Table S1 Local strains and Poisson's ratios of GWF/PDMS composites measured by optical images when loaded at two different angles.

Applied strain	0%	1%	2%	3%	5%
Global strain (0°)	0%	1.03%	2.07%	3.09%	5.06%
Poisson's ratio (0°)	--	0.46	0.47	0.47	0.47
Global strain (45°)	0%	1.05%	2.04%	3.02%	4.99%
Poisson's ratio (45°)	--	0.46	0.47	0.47	0.47
$\varepsilon_{0°}$ in 0° GTs	0%	1.03%	2.07%	3.09%	5.06%
θ'	45°	44.68°	44.30°	43.83°	42.70°
$\varepsilon_{45°}$ in 45° GTs	0%	0.45%	0.78%	0.96%	1.02%
$\frac{\Delta R_{0°}}{R_{00°}} : \frac{\Delta R_{45°}}{R_{045°}}$ **(calculation)**	--	2.24	2.58	3.12	--
$\frac{\Delta R_{0°}}{R_{00°}} : \frac{\Delta R_{45°}}{R_{045°}}$ **(experimental)**	--	2.35	2.72	3.39	--

Based on the direction and geometry of GTs, equivalent and simplified circuit models of GWF/PDMS composites were built to analyze the resistance change of composites (Figure S4). The global strains in the composite were evaluated by measuring the length changes of white squares (shown in Figure S3) using the software ImageJ. The Poisson's ratios were calculated based on the measured lengths and widths of the white square, which were compared with the theoretic value of PDMS, 0.48.[S1] The strain applied to the composite is ε, while the local strains of GTs in the two units, $\varepsilon_{0°}$ and $\varepsilon_{45°}$, were obtained by analyzing the shape changes in GTs, as shown in Table S1. The normalized resistance changes $\Delta R/R_0$ in GWFs were calculated based on the following equations:

For tension applied at 0° to GTs:

$$R_{10} = n_1 \cdot r_{10}/m_1 = L \cdot r_0/w, \quad \text{(S1)}$$

$$r_{1s} = r_0 + k \cdot \varepsilon_{0^\circ}; \quad \text{(S2)}$$

$$R_{1s} = n_1 \cdot r_{1s}/m_1 = L \cdot r_{1s}/w; \quad \text{(S3)}$$

$$\frac{\Delta R_{0^\circ}}{R_{0\,0^\circ}} = \Delta^{R_1}\big/R_{10} = (R_{1s} - R_{10})/R_{10} = \big(r_{1s} - r_0\big)\big/r_0 = \Delta r_1/r_0 = k \cdot \varepsilon_{0^\circ}. \quad \text{(S4)}$$

For tension applied at 45° to GTs:

$$R_{20} = n_2 \cdot r_0/m_2 = L \cdot r_0/w; \quad \text{(S5)}$$

$$r_{2s} = r_0 + k \cdot \varepsilon_{45^\circ}; \quad \text{(S6)}$$

$$R_{2s} = n_2 \cdot r_{2s}/m_2 = L \cdot r_{2s}/w; \quad \text{(S7)}$$

$$\frac{\Delta R_{45^\circ}}{R_{0\,45^\circ}} = \Delta^{R_2}\big/R_{20} = (R_{2s} - R_{20})/R_{20} = \big(r_{2s} - r_0\big)\big/r_0 = \Delta r_2/r_0 = k \cdot \varepsilon_{45^\circ}. \quad \text{(S8)}$$

where $R_0, R_s, \Delta R$ are the resistances before and after tension, and resistance change of GWF/PDMS composites; $r_0, r_s, \Delta r$ are the resistances before and after tension, and resistance change of GTs, respectively; L and w are the length and width of GWFs; n and m are the numbers of the units in the length and width directions, respectively. According to the calculation, the normalized resistance changes of GWF/PDMS composites with different GT orientations depend on local strains of GTs arising from the deformation in the composite.

S3. Calculation of the local strain in GTs with different orientations

The relationship between the strain applied to the composite, ε, and the local strains in GTs were established using the strain transformation equation:

$$\varepsilon_\theta = \frac{\varepsilon_x + \varepsilon_y}{2} + \left(\frac{\varepsilon_x - \varepsilon_y}{2}\right)\cos 2\theta + \frac{\varepsilon_{xy}}{2}\sin 2\theta \quad \text{(S9)}$$

where ε_x and ε_y are strains along the x- and y-directions, respectively, and ε_{xy} is the shear strain. Under uniaxial tension,

$$\varepsilon_x = \varepsilon \quad \text{(S10)}$$

$$\varepsilon_y = -v\varepsilon \quad \text{(S11)}$$

$$\varepsilon_{xy} = 0 \quad \text{(S12)}$$

When the loading direction is the same as the GT direction, the local strain in GTs is given by:

$$\varepsilon_{0^\circ} = \varepsilon_x = \varepsilon \quad \text{(S13)}$$

When the loading direction is 45° to the GTs, the local strain in GTs is given by:

$$\varepsilon_{45^\circ} = \frac{\varepsilon - v\varepsilon}{2} + \left(\frac{\varepsilon + v\varepsilon}{2}\right)\cos 2\theta' = \left(\frac{1-v}{2} + \frac{1+v}{2}\cos 2\theta'\right)\varepsilon \quad \text{(S14)}$$

where θ' is the angle between the GTs and the loading direction after loading. The external load induced the shape change of the orthogonal structure of GTs, leading to the change of angle between GTs, as shown in Figure S3. The angle between the GT and the loading direction after loading is obtained by the geometric relationship:

$$\tan\theta' = \frac{1 - v\varepsilon}{1 + \varepsilon} \quad \text{(S15)}$$

S4. Cyclic performance of GWF/PDMS composites

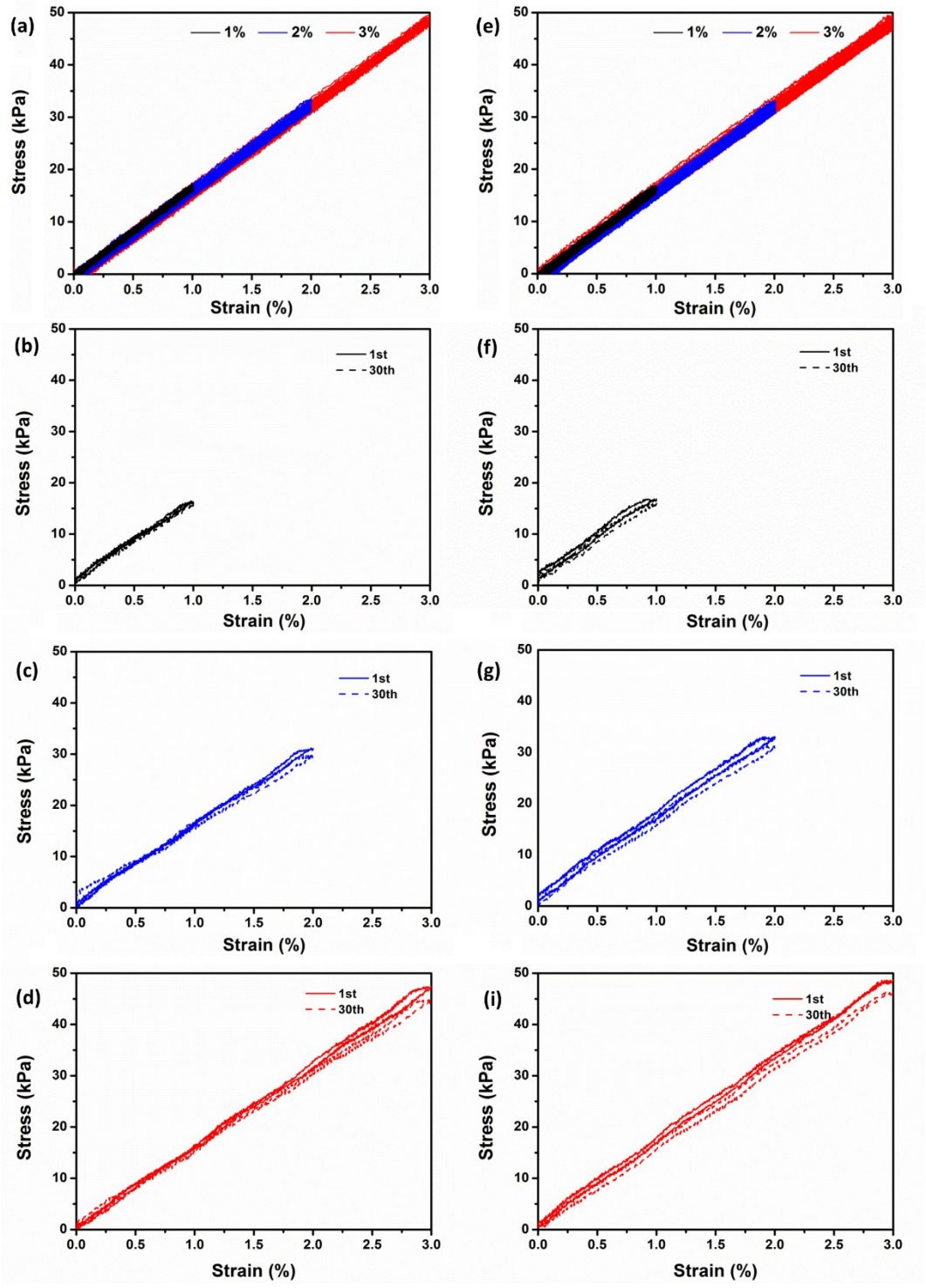

Figure S5 Stress-strain curves of GWF/PDMS composites with (a) GTs (0°) and (e) GTs (45°). Strain-stress curves of GWF/PDMS composites with (b-d) 0° GTs and (f-i) 45° GTs in the first and 30th cycles at different strains.

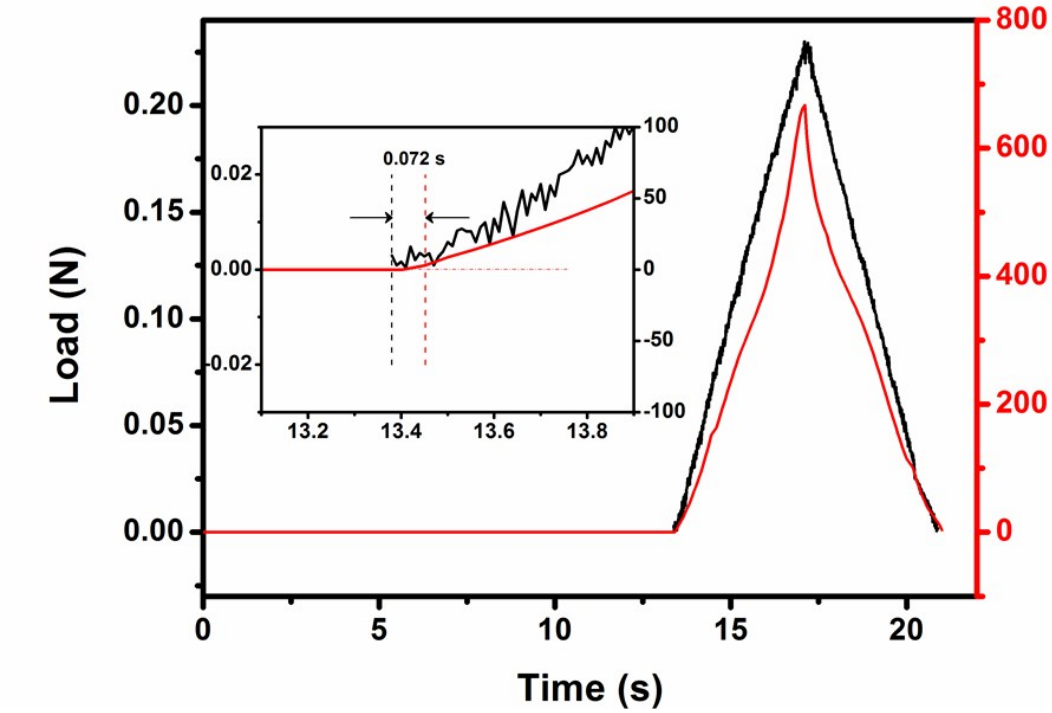

Figure S6 The response time of composite to 3% tensile strain.

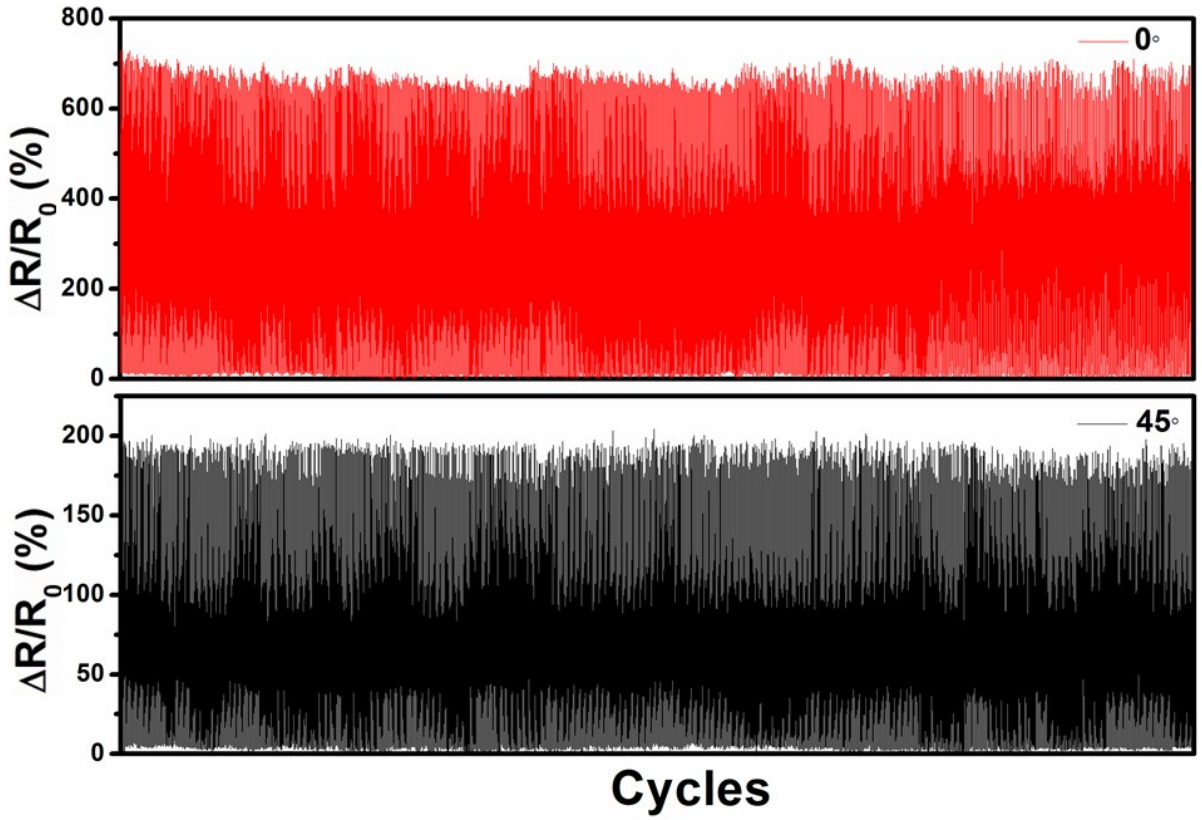

Figure S7 Normalized resistance changes of GWF/PDMS composites for 1000 cycles at 3% strain.

S5. Calculation of resistance change of composite under bending test

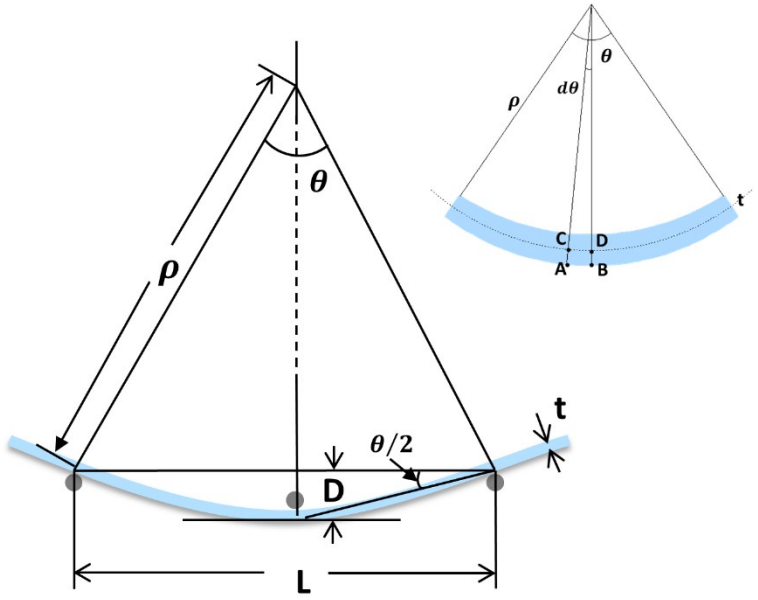

Figure S8 Geometry of composites during three-point bending.

The three-point bending model is established using the "Euler-Bernoulli beam theory" for t ≪ L (t/L=1/50) to analyze the strain distributions in the composite. The composite is bent from a flat plane to an arc with a bending curvature 1/ρ and a bending angle θ, and the maximum flexural strain in the center ε_{max}. ε_{max} is given by:

$$\varepsilon_{max} = \frac{AB - CD}{CD} = \frac{(\rho + t/2)d\theta - \rho d\theta}{\rho d\theta} = \frac{t}{2\rho} \tag{S16}$$

ρ and θ are given by:

$$\sin\frac{\theta}{2} = \frac{L}{2\rho} = \frac{D}{\sqrt{D^2 + L^2/4}} \tag{S17}$$

where t is the thickness of GWF/PDMS composite, D and L are the deflection and the span in three-point bending, respectively.

S6. Fabrication and test of wearable GWF/PDMS composites sensors

Figure S7 shows the fabrication process of wearable sensors. To prepare sensors that can be easily mounted on fingers, an H-shaped acrylic mold was prepared by laser cutting. A ~1 mm thick GWF/PDMS composite sensor with two copper wires connected was embedded within the PDMS matrix to form a sandwich structure. With the 3D printed buckles installed at the ends, the semi-transparent H-shaped sensors could be easily mounted on fingers with adjustable lengths.

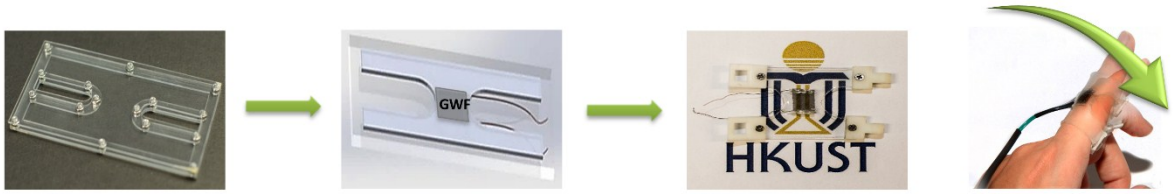

Figure S9 Schematic flowchart of the fabrication process of wearable sensors.

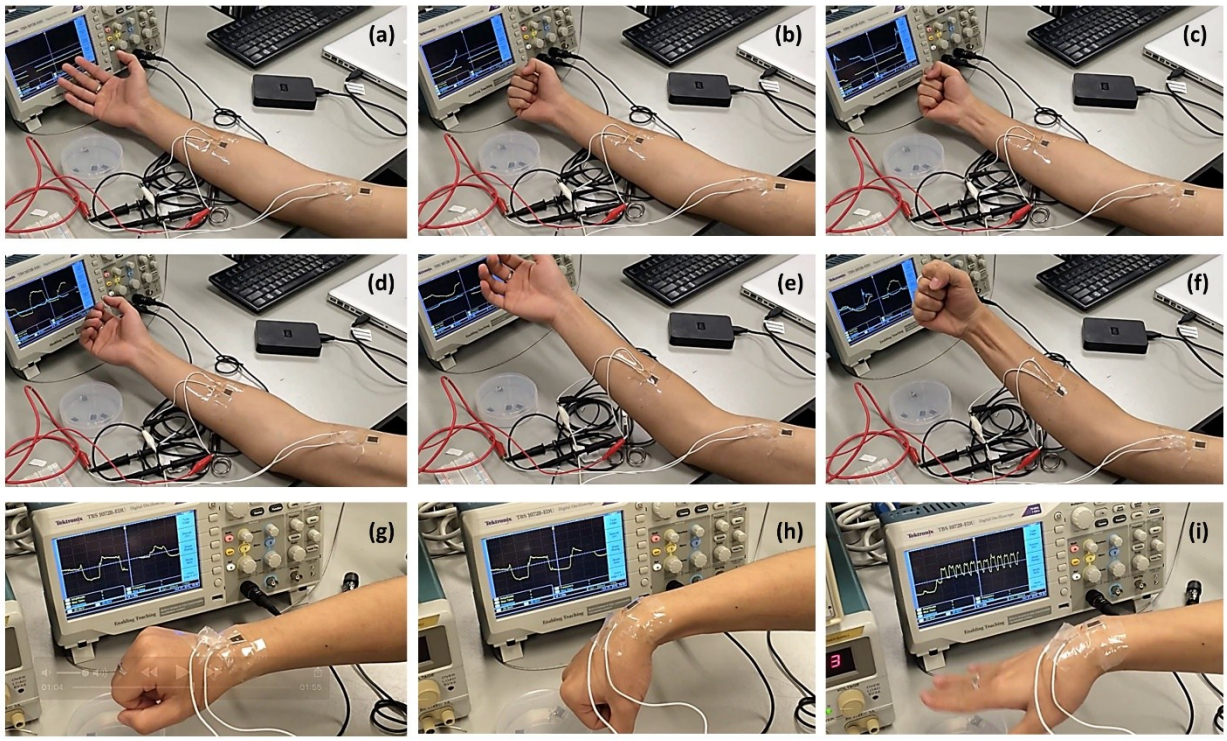

Figure S10 Measurements of resistance changes of composite sensors on (a-f) forearm and posterior arm, and (g-i) wrist.

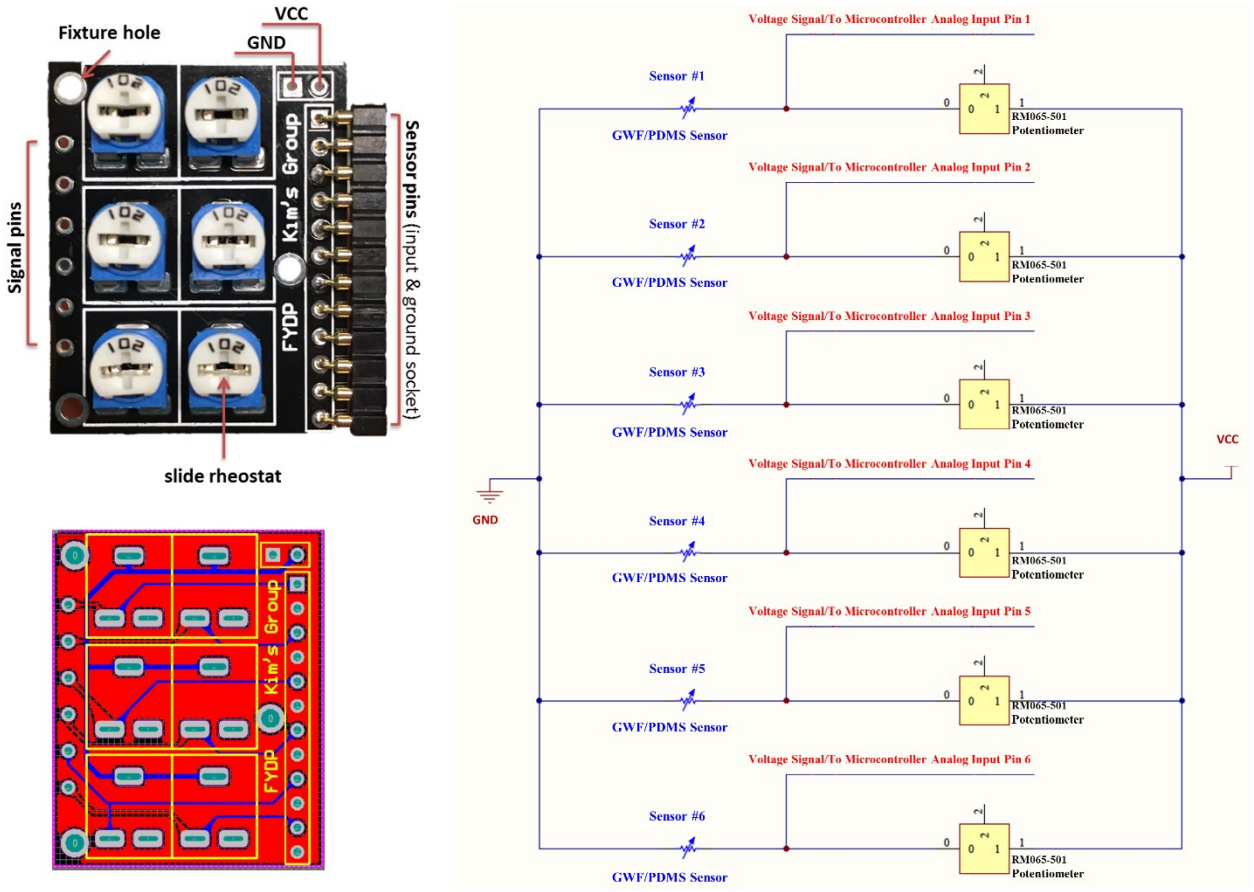

Figure S11 Photograph of custom-designed printed circuit board (PCB)

S7. The working mechanism of Musician App on smartphone

Music was played with a java class Jetplayer by queueing and controlling several MIDI (Musical Instrument Digital Interface) files synchronized with multiple sensors into the jet files. Jet interactive Engine (JET) is broadly used in the game music on many small devices, supporting a flexible music format that creates extended musical sequences with a minimal amount of data. MIDI files contained various functions of music, such as notation, pitch, velocity, volume, vibrato, audio planning, cues, and clock signals. The sequencing was fixed at the time, and the music file was authored through a developer's application, the SONiVOX JETCreator, which can be changed

dynamically under the program controlled by the output signals arising from the body motion sensors.

S8. The measurement of wrist pulse

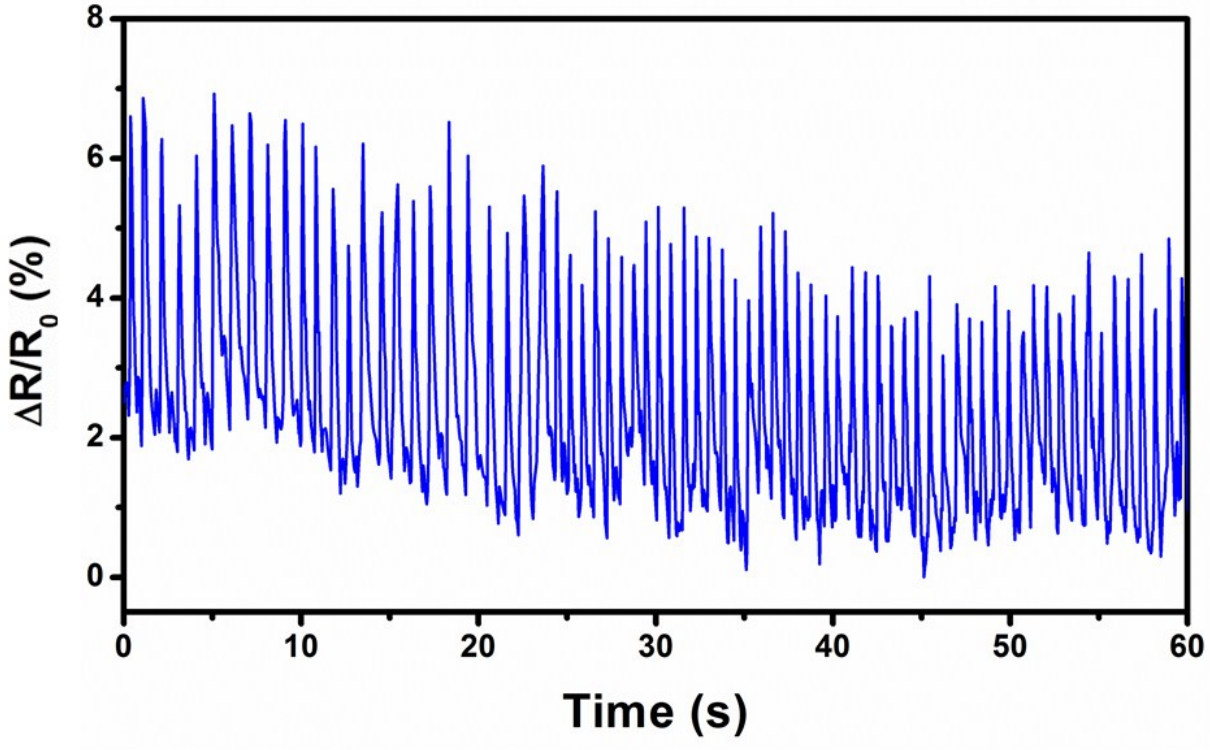

Figure S12 Normalized resistance change of composite sensor arising from wrist pulse for 1 minute. The pulse rate is 74 per minute.

Videos:

1. Video 1: Response sensitivity test of composite sensors_1.
2. Video 2: Response sensitivity test of composite sensors_2.
3. Video 3: Response sensitivity test of composite sensors_GTs orientations.
4. Video 4: music - Ode to Joy.
5. Video 5: music - Jingle Bells.

[S1] N. Bowden, S. Brittain, A. G. Evans, J. Hutchinson and G. M. Whitesides, *Nature*, 1998, **393**, 146-149.